Proceedings, 7th African Rift Geothermal Conference
Kigali, Rwanda 31st October – 2nd November 2018

1D and 2D Inversions of Magnetotelluric Data from Butajira Geothermal Field, Southern Ethiopia

Andarge Mengiste, Kebede Mengesha, Getachew Burussa, Fitsum Abera, Assefa Yismaw, Tsegaye Wondifra

Geological Survey of Ethiopia, P.O. Box 469, Addis Ababa, Ethiopia.

andmeng@gmail.com

Keywords:

1D inversion (Levenberg-Marquardt), 2D_Occam inversion, MT, Butajira prospect

ABSTRACT

Butajira geothermal field is located in the western escarpment of the Central Main Ethiopian Rift (CMER) within the Ethiopian sector of the East African Rift System (EARS) that is believed to have independent heating and circulation system. It is a newly discovered prospect among the 23 prospects that are thought to have high enthalpy resource. Inversion is a process to determine the model parameters from data. There are many inversion algorithms that have been introduced and applied in Geophysical problems; among these we have used Levenberg-Marquardt (LM) algorithm for 1D case; for 2D case (2D_Occam inversion algorithm). One-dimensional (1D) and two-dimensional (2D) Magnetotelluric (MT) data inversions were conducted to reveal the subsurface resistivity structure beneath the south eastern part of Butajira prospect (known as Ashute plain), Ethiopia. Twenty-seven Magnetotelluric sounding data spanning four lines of investigation were inverted. The result depicts three main resistivity layers. The first one is a low resistive surface layer (< 10 Ωm) of up to about 1.5 km depth which can be correlated with alteration zones caused by geothermal activity or lacustrine sediments or hydrothermally altered clay cap. Below this low resistive layer, resistivity increases up to (10-60 Ωm). This indicates an advancement to a possible reservoir at depth below about 1 km with a thickness of up to 1.5 km. The third one beneath the thick high resistivity layer is a deep conductor that could be associated with heat source. The faults are inferred on the profiles 1, 2 and 3 which could be considered as the pathways for the geothermal fluids.

1. Introduction and background

Ethiopia started long-term geothermal exploration in 1969. Over the years, an inventory of the possible resource areas within the Ethiopian sector of the EARS has been built up. On the basis of several years of geothermal exploration activities about 120 localities have been

identified within the Rift System that is believed to have independent heating and circulation system, about 23 prospects are thought to have potential for high enthalpy resource development, including for electricity generation and direct uses (UNDP, 1973). The explored prospects in the country (Kebede, S., 2015) are at various stages of exploration starting from regional assessment to advanced (development stage). The study area is located within this system, bounded by the western escarpment of the CMER showing different geothermal manifestations. It is the new prospect among the 23 geothermal prospects that are found throughout the Ethiopian Rift System (ERS). The prospect is under first stage of surface exploration and has been inspected for the near surface soil temperature survey, surface geological mapping, geochemical and geophysical (MT and Magnetic surveys) studies from February-March 2017 GC which is the first survey in its kind (Abera, B., and Mulugeta, N., (2017). For 1D case, we used the Levenberg-Marquardt non-linear least square inversion (Widodo and Saputera, D.H., 2016). According to this inversion scheme the misfit function is the root mean square difference between measured and calculated values. The program offers the possibility to keep models smooth, both with respect to resistivity variation between layers and layer thicknesses. For 2D case, we used 2D_Occam inversion which was first introduced by Hedlin and Constable (1990). Since then the Occam's inversion has been widely used to interprate electromagnetic data including Magnetotelluric data. This inversion scheme produces a smooth model that fits a data sets within certain tolerances. By using smoothness (roughness), an inverted model yields the best fit to the data.

1.1 Scope and objective of the study

The objective of the survey was to acquire the high resolution Magnetotelluric data over the survey area in order to: (i) obtain a model of the subsurface resistivity structure of the Butajira geothermal field, (ii) estimate the probability of occurrence, extension and depth of the geothermal reservoir and possible recharge zones for the system and (iii) advance the state of knowledge of the prospect to one level. The scope of the study includes: data acquisition, processing, inversion and modelling, result and discussion and conclusion and recommendation.

1.2 The survey area

The Butajira geothermal field is located in the western escarpment of the CMER that extends from Afar (northern Ethiopia) to Kenya and belongs to the EARS. Butajira town is 135 km south of Addis Ababa and the geophysical survey area is about 20 km south east of Butajira town. Morphologically, the prospect can be categorized (Abera, B., and Mulugeta, N., (2017) into two: (i) the western escarpment area which is characterized by: pyroclastic deposits, flood basalts, basement rocks and the vertical cliffs of high mountain range rising over 2500 m a.s.l and the second one is the down thrown block (the rift floor) which is characterized by: talus deposits, fan deposits, alluvial and calluvial deposits lacustrine sediments and geothermal manifestations (hot spring, mud pool, occasional geyser and geothermal grass). Hydro-geologically, the prospect is rich in ground water resource that drains from the rift shoulder and the escarpment area is believed to be the major source of recharge to geothermal reservoirs in the rift floor and the quaternary sediments in the rift floor serve as impermeable cap to convective heat flow system in the basin.

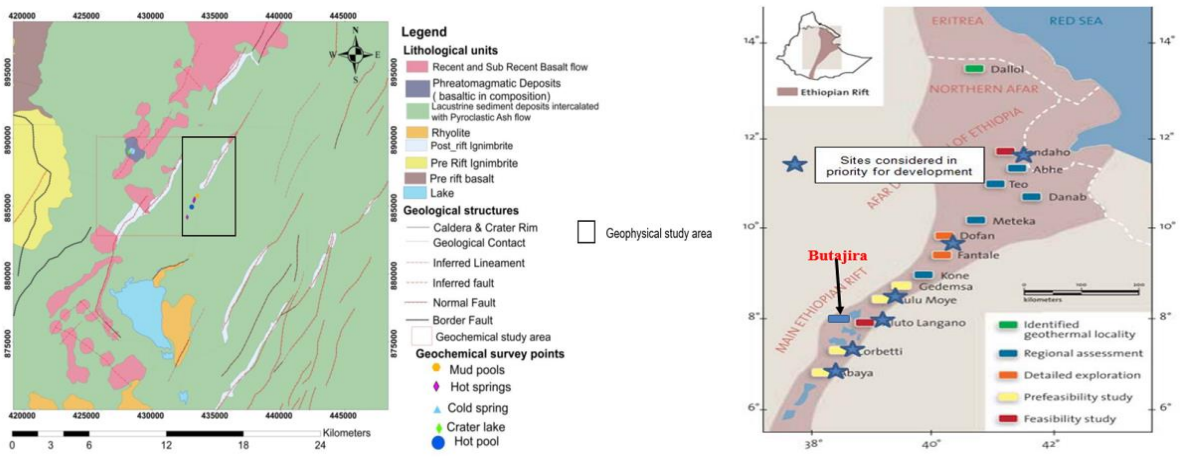

Figure 1. Geological map of the study area (modified by Yafet Gebrewold after Zelalem Abebe and Yared Sinetibeb, 2017) and location of Butajira prospect.

2 The Magnetotelluric method

The Magnetotelluric (MT) method is a natural source electromagnetic method developed in 1950s by Tikhonov (1950) and Cagniard (1953) to image the Earth's subsurface by measuring the natural variations in electrical and magnetic fields within the Earth's surface. The investigation depth ranges from the shallow zone where higher frequencies are recorded down to 5000 m or deeper with long period soundings. The MT method employs the fluctuations in the Earth's magnetic field which induce electrical currents in the Earth. The fluctuations are mainly derived from two origins. High frequencies (>1 Hz) occur mainly due to world-wide thunderstorm activity, usually near the equator, while low frequencies (<1 Hz) occur mainly due to complex interaction between the solar wind (ionized particles) and the Earth's magnetic field. The ratio of electrical and perpendicular magnetic field variations can be treated as a kind of impedance and is linked to the electrical conductivity of the penetrated structures (by measuring impedance in various frequency bands, it is possible to obtain the resistivity structure of the subsurface to the significant depths). Since the attenuation of electromagnetic fields depends on their frequency (and the electrical conductivity of the media) a depth sounding can be achieved by analyzing the electrical and magnetic fields at certain frequencies, measured at a surface. Thus the measured data can be processed and displayed as sounding curves of apparent resistivity versus frequency or (alternatively) period). As with other geo-electric measurements the MT data can then be converted to resistivity and depth by the use of the inversion algorithms. The involved model may be 1D (horizontal layered earth, i.e. resistivity changes with depth only), 2D (in addition to 1D a variation of resistivity also in one horizontal direction is allowed or 3D (resistivity may change in all the three spatial directions). Some aspects of processing and inversion are treated in the following paragraph.

2.1 Details on MT data acquisition

Before starting the MT data acquisition, all the box (instrument) and coil calibration had been taken place at the remote reference site. For MT data acquisition, three MT units were being used, two of them were rovers whereas one was the reference station which has 20 km areal distance from the survey area, each system consists of a 5 channel data logger (MTU-5A) manufactured by Phoenix Geophysics Company Canada. A total of, 32 MT sampling stations were collected on a rectangular grid of profile and station interval of 1 km each. The measuring equipments have been set up to measure two components of electric signals

(normally in the NS and EW directions) and three components of magnetic signals (NS, EW and vertical directions). Two electric field dipoles were formed by four non-polarizable electrodes (electric field sensors). In most cases the electric field sensors had been placed into a bentonite slurry to yield low contact resistance between the electrode and the ground. Dipole length was generally 100 m, but in unfavorable terrain (rugged and steep) conditions 50 m. All magnetometers were buried into the ground to prevent any movement of them (or from wind induced noise). Power supply to each station was granted by 12 Volt batteries, providing sufficient energy for about 20 hours of continuous operation. A grounded electrode was also used to prevent any damage to the instrument as shown in figure 2.

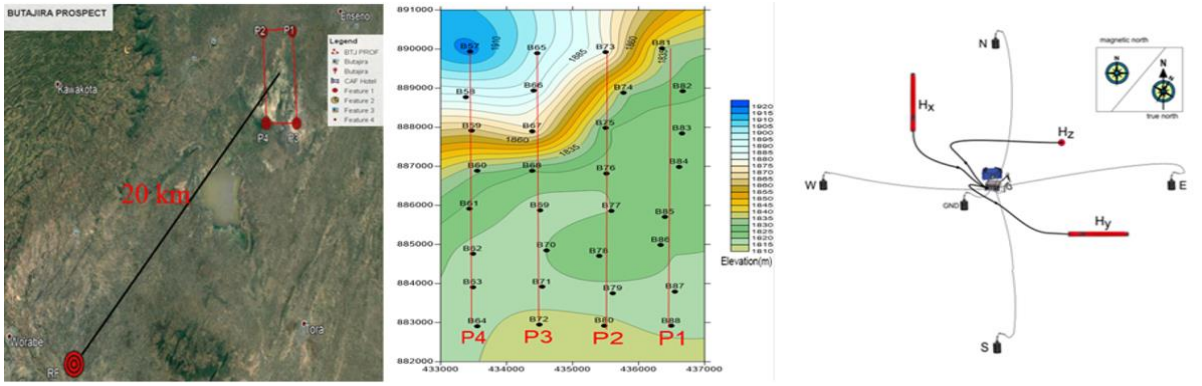

Figure 2. Location of MT remote reference station relative to observation points and schematic set up of MT survey layout.

Since the MT method utilizes natural electromagnetic fields, if there are artificial structures that use electricity in the vicinity of the survey area, then the observed data are often contaminated by the electromagnetic noise generated by them. It is difficult to distinguish between the natural signals and the noises only with data at one MT site. Therefore, by setting the remote reference site at quiet place that is sufficiently far away, observing the time series data of the electromagnetic fields at the same time at the measurement site in the survey area, and using the signal commonly included in both of them preferentially, we can remove the local noise at the measurement site by using the remote reference processing. Therefore, the study area and the reference site were operated simultaneously at different locations under a fully recording time of GPS clock. So all the data of the survey area have been remote reference processed corresponding to the reference site. To ensure acceptable data quality for latter processing and interpretation it is strongly recommended to inspect recorded data on-site and perform preliminary time series processing in the field camp on a daily basis.

2.2 Details on MT data processing, data quality and static shift correction

2.2.1 Details on MT data processing

Out of 32 MT soundings, 27 of them were processed and used for the interpretation. The time series data were downloaded from the compact flash card of MTU-5A units. The first step in time series processing is the visual inspection of the recorded data using the Synchro Time Series Viewer program. This program allows for imaging and printing of graphical representations of the raw time-series data, it computes power spectra densities derived from the time-series data and coherence between pairs of orthogonal channels. A processing overview is given in fig. 5. The green part is referred to as time series processing performed by the SSMT 2000 Software and MT editor from Phoenix Geophysics Company and the red

part is referred to as inversion performed by the 1D Marquardt (developed by Professor Mizunaga Kyushu University) and 2D Occam's inversion (Hedlin and Constable, 1990).

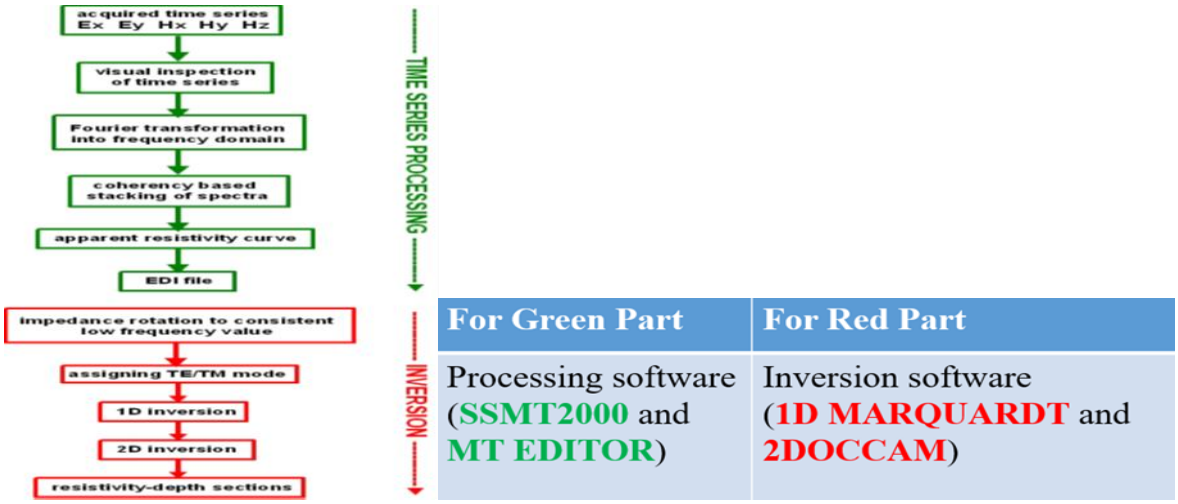

Figure 3. MT processing and inversion flow.

During processing, the SSMT 2000 program takes input raw time series data, calibration files, and site parameter files. Then in an intermediate step, it produces Fourier coefficients, which are then reprocessed with data from reference sites, using robust routines. The output are MT plot files (MTH and MTL) containing multiple cross powers for each of the frequencies (where H and L stand for high and low). The program MT-editor takes the output from SSMT2000 program and displays resistivity and phase curves as well as the individual cross powers that are used to calculate each point on the curve. Cross powers that were affected by noise can be automatically or manually excluded from the calculation. Then, the impedances from the five frequency bands are put together and saved in the internationally adopted EDI (Electronic Data Interchange) file format.

2.2.2 Data quality

Most of sounding data are of medium quality and can be used for interpretation up to 100 s period lengths. Some stations within the survey area were affected by ground movement and noise owing proximity to local villages and nocturnal wild animal activity, and the local power grid.

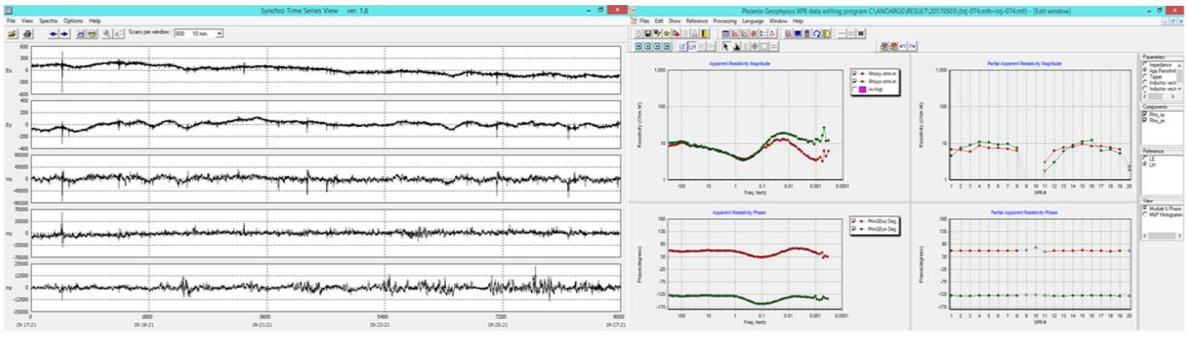

Figure 4. Example of raw and processed MT data of station number of BTJ074.

2.2.3 Static shift correction

A static shift occurs because of near surface resistivity in-homogeneities and topographic effects. It is due to electric field distortion because of the dependency of electric field on the

resistivity of the material where the voltage difference is measured. Static shift, has been observed on a few stations only and has been removed by means of Average Statistical Method namely, Spatial Median Filter Method.

3 Inversion and modelling

Geophysical data is modelled and interpreted in terms of subsurface geology in two ways: a direct way, known as forward modelling, and indirect way, known as inverse modelling. In the forward method, the model parameters of the subsurface geology are estimated from geophysical observations and response functions. On the other hand, in the inverse method a model of the subsurface is assumed and a theoretical geophysical response is computed for the assumed model and compared with the observed data. This process is repeated for various models through an iterative response until a minimum difference between the computed and observed responses is achieved.

3.1 1D inversion and modelling of MT data using Levenberg-Marquardt scheme

The inversion algorithm used in this program is based on the Levenberg-Marquardt, a non-linear least square method (1D Marquardt) developed by Professor Mizunaga. The misfit function is the root-mean-square difference between measured and calculated values. The program offers the possibility to keep models smooth, both with respect to resistivity variation between layers and layers thicknesses. The Levenberg-Marquardt Algorithm (Widodo and Saputera, D.H., 2016) is an algorithm that applies the minimization of model perturbation to the Gauss Newton solution. It can be done by minimizing the objective function F.

$$F = (\mathbf{d} - g(\mathbf{m_0} + \Delta\mathbf{m})) + \lambda||\Delta\mathbf{m}||^2 \quad (1)$$

where F is objective function, **d** is data (apparent resistivity or phase), g is forward operator that relates the model parameter with its response, **m** is solution models, $\Delta\mathbf{m}$ is model parameter updates, $\mathbf{m}_0$ is initial model and λ is a parameter that shows the effect of model perturbation. Figure below shows an example of estimated model from geophysical observations and response functions. There is a good overlapping between the observed (the determinant) and the calculated one.

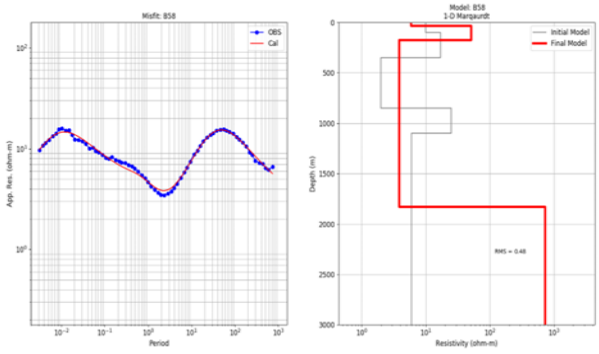

Parameter	Initial	Final	Fix
rho 1	10	6	0
rho 2	17	51.3	0
rho 3	2	3.86	0
rho 4	25	729	0
rho 5	6	2.15	0
thic 1	100	34.5	0
thic 2	250	141	0
thic 3	500	1654	0
thic 4	250	10140	0
Iteration	16		
RMS	0.48		

Figure 5. Estimated model of station B58 along profile p4.

3.2 2D_Occam inversion and modelling of Magnetotelluric data

For 2D case, we used 2D_Occam inversion which was first introduced by Hedlin and Constable (1990). Since then the Occam's inversion has been widely used to interpret electromagnetic data including Magnetotelluric (MT) data. This inversion scheme produces a

smooth model that fits a data sets within certain tolerances. By using smoothness (roughness), an inverted model yields the best fit to the data. The 2D_Occam inversion is an expansion of 1D_Occam inversion. At k-th iteration, the estimated model parameters are obtained by solving the following equation:

$$\mathbf{m}_{k+1} = [\mu (\partial_y^T \partial_y + \partial_z^T \partial_z) + (\mathbf{WJ}_k)^T \mathbf{WJ}_k]^{-1} (\mathbf{WJ}_k)^T \mathbf{W} \qquad (2)$$

where **m** is matrix of model parameters, k is number of iteration, μ is Lagrange multiplier, ∂_y is roughness matrix to describe different model parameter laterally and ∂_z is roughness matrix to describe model parameter vertically, T represents transpose of matrix, W is weighted diagonal matrix, and J is Jacobian matrix. Figure below shows an example of best fit of estimated model of TE and TM modes

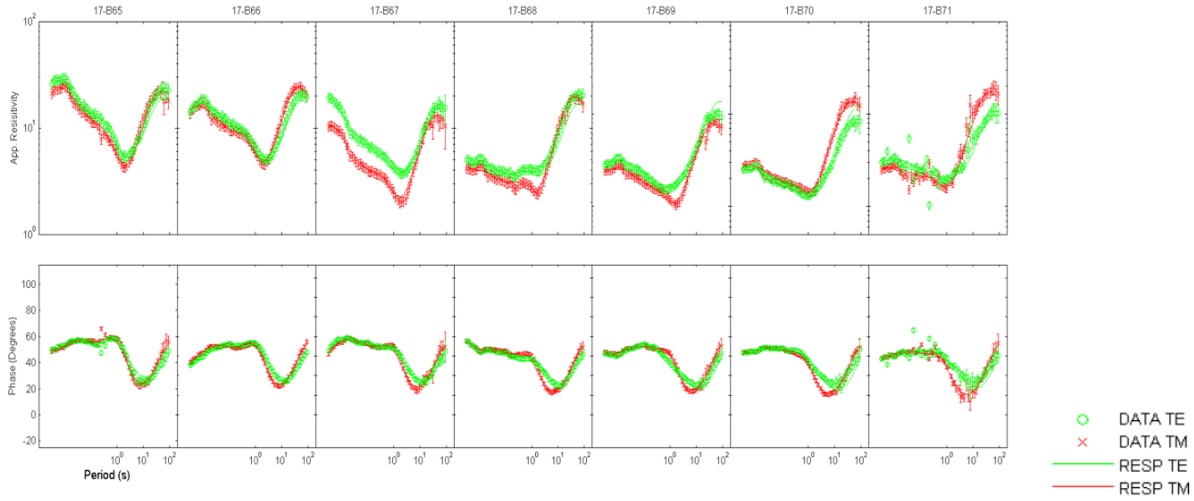

Figure 6. Best fit of TE and TM modes along profile p4.

The off diagonal elements of the impedance tensor are used to calculate apparent resistivity and phase curves for the two perpendicular orientations: XY = North component of the electric field (Ex) and East component of the magnetic field (Hy), YX = East component of the electric field (Ey) and North component of the magnetic field (Hx). For further processing the impedance tensor is rotated mathematically by a constant angle derived from the swift angle at low frequencies. If the subsurface is 2D, the electromagnetic (EM) fields are usually polarized into two modes referred to as TE-mode when the E fields are parallel to the direction of strike and the TM-mode when the H-field is parallel to the strike direction. Both, TE- and TM- modes are taken into account in the 2D modelling. When the MT polarization is in the direction of the regional strike (figure 9), it is assumed that there will be no conductivity variation in this direction and the resistivity varies only with depth and along one lateral axis (2-D). In this case the EM fields decouple into 2 distinct polarizations, the TE (transverse electric) and TM (transverse magnetic). During data acquisition, the EM measurements are usually made in the NS and EW directions which do not always correspond to the direction of strike. MT data interpretation therefore involves the decomposition of the EM fields so that data can be reduced to a form that satisfies the 2-D assumptions for the commonly used 2D interpretation methods.

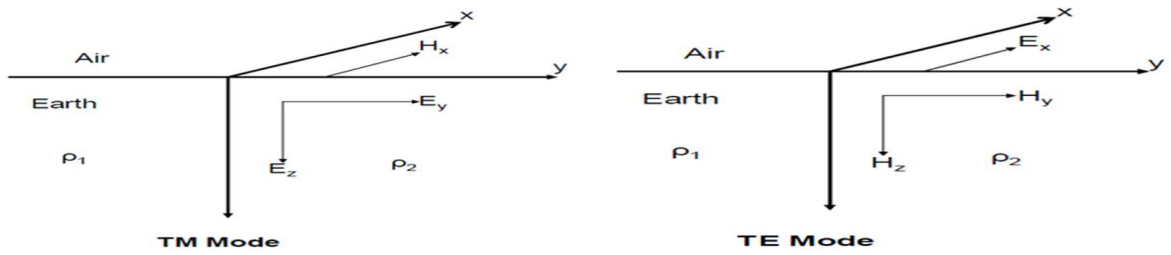

Figure 7. The effect of 2D half space. In the TE mode, the current is polarized in the direction of strike X creating associated magnetic fields in the Y and Z directions. In TM mode, the magnetic field is along strike direction generating associated electric fields in the Y and Z directions.

4 Results and discussions

The 1D and 2D inversions were carried out. The sounding locations were assigned to four profiles oriented almost N-S, namely P1, P2, P3 and P4. Both 1D and 2D models are the outcome of a processing and inversion procedures as briefly explained in the above sections. To compare all the MT resistivity sections and models easily, the same scaling has been considered for all profiles.

4.1 1D Marquardt inversions

4.1.1 Profile line p1

The figure shows resistivity profile resulted from 1D inversion for the first section. This profile consists of seven MT sounding locations with a lateral length of 7.1 km and depth range of about 4.82 km. The 1D inversion result shows a very low resistive surface layer (<10 Ωm), covering the lateral distance of the all profile, with a layer thickness various from about 300 m to -500 m. This may be correlated with alteration zones caused by geothermal activity or with lacustrine sediments or with hydrothermally altered clay cap. Resistivity increases with depth, up to about 10-60 Ωm. This can be interpreted as an advancement to the deeper reservoir, whose elevation varies approximately from 1000 m to -2000 m. Generally, in geothermal areas, the clay cap layer possesses low resistivity value of less than or equal to 10 Ωm (Pellerin et al., 1996), whereas reservoir typically exhibits higher resistivity value of about 10-60 Ωm.

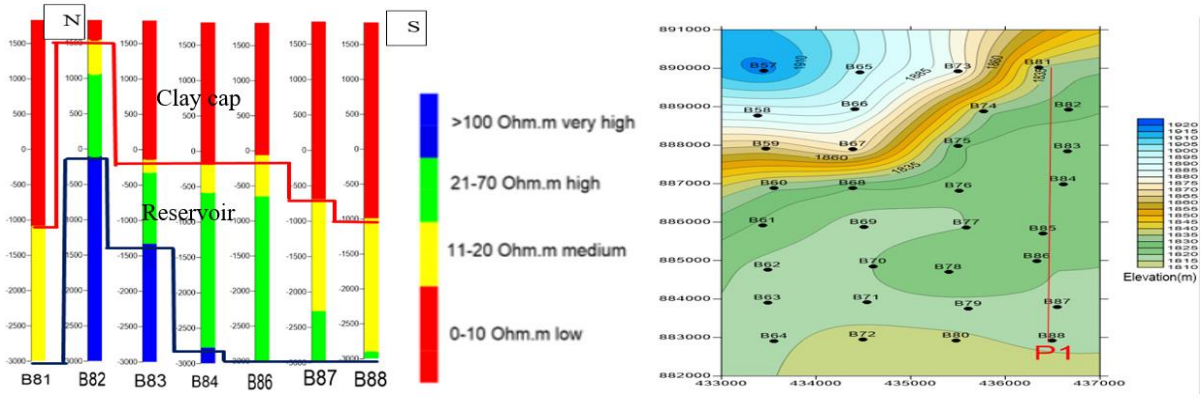

Figure 8. Location of MT soundings and 1D Marquardt inversion result along the profile p1.

4.1.2 Profile line p2

This profile contains seven MT soundings with a lateral length of 7 km and the depth range of 4.83 km. Similar to profile number one, an extremely low resistive surface layer (<10 Ωm)

is present throughout the profile having a thickness of up to -500 m. This may be correlated with alteration zones caused by geothermal activity or with lacustrine sediments or with hydrothermally altered clay cap. Resistivity increases with depth up to about (10-60) Ωm. This can be interpreted as an advancement to the deeper reservoir whose elevation varies approximately from 500 m to -1500 m.

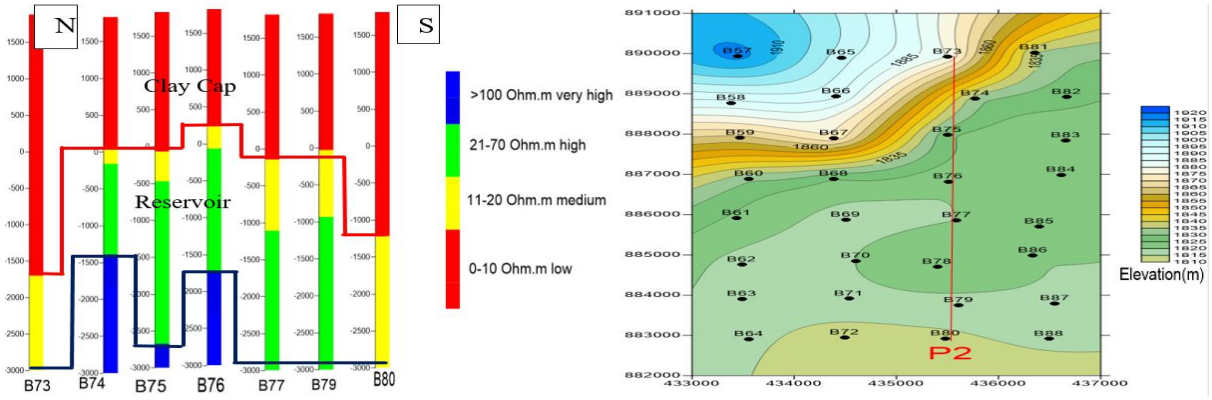

Figure 9 Location of MT soundings and 1D Marquardt inversion result along the profile p2.

4.1.3 Profile line p3

This profiles contains seven MT soundings with a lateral length of 6 km and depth range of 4.85 km. Similar to other profiles, here is also the low resistive surface layer (<10 Ωm) is present from station number B67 to B71, having a thickness of up to -1400 m. This may be correlated with alteration zones caused by geothermal activity or lacustrine sediments or hydrothermally altered clay cap. The first layers of stations B65 and B66 have relatively higher resistivity, with a thickness that varies from 300 m to 1300 m). This is can be correlated with recent and sub recent basaltic flow or due to volcanic over burden. As we go down, resistivity increases with depth up to about (10-60) Ωm. This can be interpreted as an advancement to the deeper reservoir whose elevation varies approximately from sea level to -2500 m.

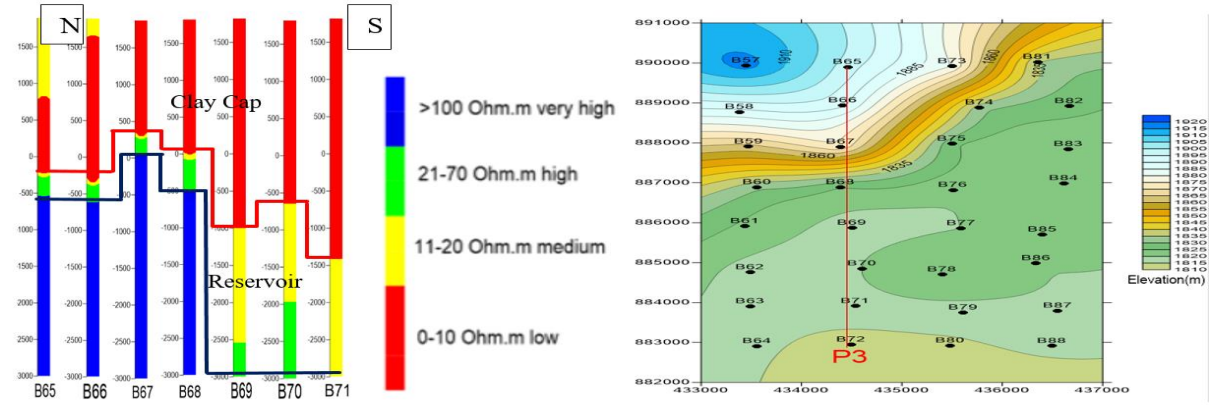

Figure 10. Location of MT soundings and 1D Marquardt inversion result along the profile p3.

4.1.4 Profile line p4

This profile contains six MT soundings with a lateral length of 7 km and a depth range of 4.85 km. Stations number B60, B62 and B63 have low resistive surface layers (<10 Ωm), similar with profile number P1 and P2. This may be correlated with alteration zones caused by geothermal activity or lacustrine sediments or hydrothermally altered clay cap having a

thickness of up to -1800 m. Whereas, for stations number B57, B58 and B64, the resistive surface layers are close to the shallower part. This is due to the recent and sub-recent basaltic flow or due to volcanic over burden. As we go down, the resistivity is increases with depth up to about 10-60 Ωm. This can be interpreted as an advancement to the deeper reservoir whose elevation varies approximately from sea level to -2500 m.

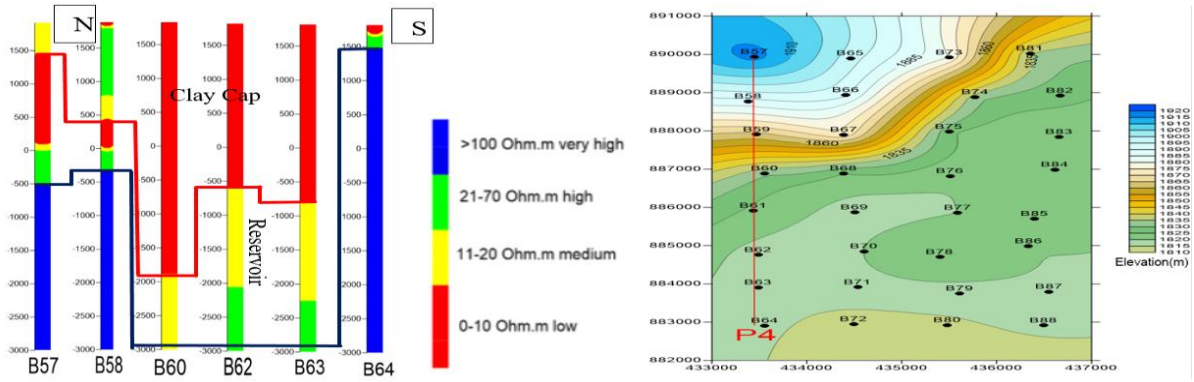

Figure 11. Location of MT soundings and 1D Marquardt inversion result along the profile p4.

4.2 2D_Occam models

4.2.1 Profile line p1

The figure shows 2D_Occam model along profile P1 resulted from 2D_Occam inversion. This profile consists of seven MT sounding locations with a lateral length of 7.1 km and depth range of about 10 km. The 2D_Occam inversion result shows a very low resistive surface layer (<10 Ωm), covering the lateral distance of the all profile, with a layer thickness various from about 1 km to 1.5 km. This may be correlated with alteration zones caused by geothermal activity or lacustrine sediments or hydrothermally altered clay cap. As we go down, resistivity increases with depth up to about 10-60 Ωm. This can be interpreted as an advancement to the deeper reservoir whose top and bottom boundary varies approximately from 1 km to 3 km respectively. In this survey, the estimated steep fault line is inferred between the boundary of conductive and resistive zone. Generally, in geothermal areas, the clay cap layer possesses low resistivity value of less than or equal to 10 Ωm (Pellerin et., 1996), whereas reservoir typically exhibits higher resistivity value of about 10-60 Ωm.

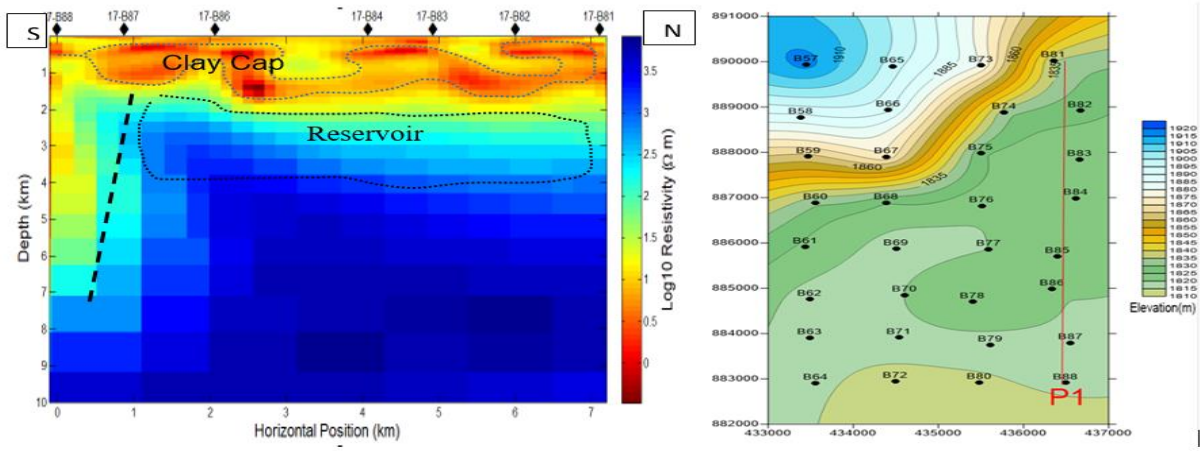

Figure 12. 2DOccam model along the profile p1.

4.2.2 Profile line p2

This profile contains seven MT soundings with a lateral length of 7 km and the depth range of 5 km. Similar to profile number one, low resistive surface layer (<10 Ωm) is present having a thickness that various from 0.5 km to 2 km. This may be correlated with alteration zones caused by geothermal activity or lacustrine sediments or hydrothermally altered clay cap. As we go down, resistivity increases with depth up to about (10-60) Ωm. This can be interpreted as an advancement to the deeper reservoir whose top and bottom boundary varies approximately from a depth of 0.5 km to 3 km. Here is also the estimated fault line is inferred between the conductive and resistive boundary.

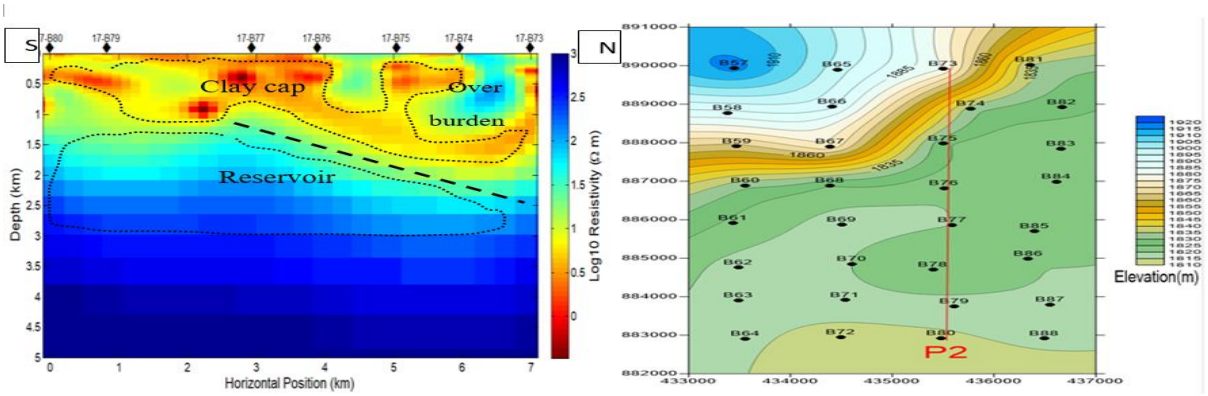

Figure 13. 2DOccam model along the profile p2.

4.2.3 Profile line p3

This profiles contains seven MT soundings with a lateral length of 6 km and depth range of 5 km. Similar to other profiles, here is also the low resistive surface layer (<10 Ωm) is present within the profile between station number B68 and B71, having a thickness that varies from 0.75 km to 1.6 km. This may be correlated with alteration zones caused by geothermal activity or lacustrine sediments or hydrothermally altered clay cap. Whereas for the shallower part of stations between B65 and B68 (which are relatively resistive with a thickness that varies from 0.25 km to 0.75 km). This is can be correlated with recent and sub recent basaltic flow or due to volcanic over burden. As we go down, the resistivity is increases with depth up to about (10-60) Ωm. This can be interpreted as an advancement to the deeper reservoir whose top and bottom boundary varies approximately from 0.75 km to 2.7 km depth. Here is also the estimated fault line is inferred between the conductive and resistive boundary.

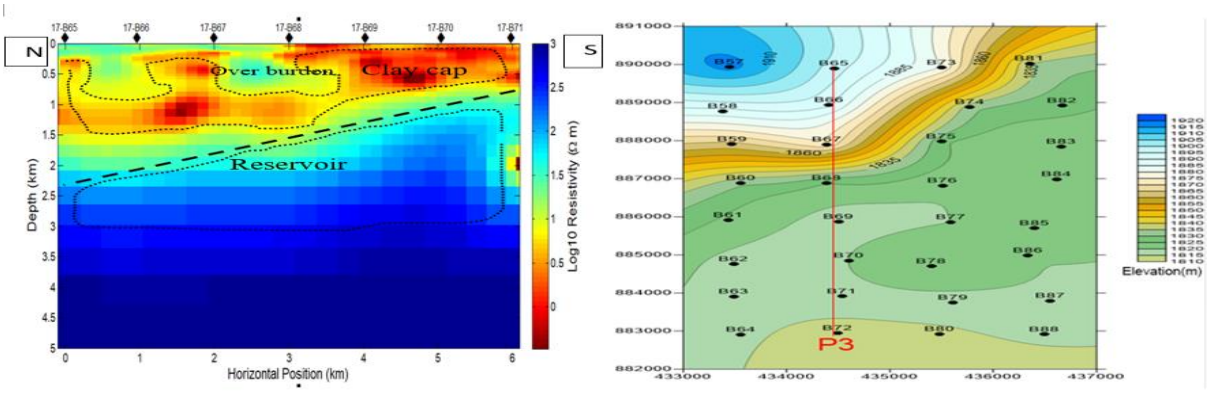

Figure 14. 2DOccam model along the profile p3.

4.2.4 Profile line p4

This profile contains six MT soundings with a lateral length of 7 km and a depth range of 5 km. Stations number B60, B62, B63 and B64 have low resistive surface layers (<10 Ωm), similar to profile number P1 and P2. This may be correlated with alteration zones caused by geothermal activity or lacustrine sediments or hydrothermally altered clay cap having a thickness of up to 1 km to 1.5 km. As we go down, resistivity increases with depth up to about (10-60) Ωm. This can be interpreted as an advancement to the deeper reservoir whose top and bottom boundary varies approximately from 1 km to 2.5 km. Whereas, for stations number B57, B58 and between B62 and B63, the resistive surface layers are close to the shallower part with a thickness that varies from 250 m to 500 m. This is due to the recent and sub-recent basaltic flow or due to volcanic over burden.

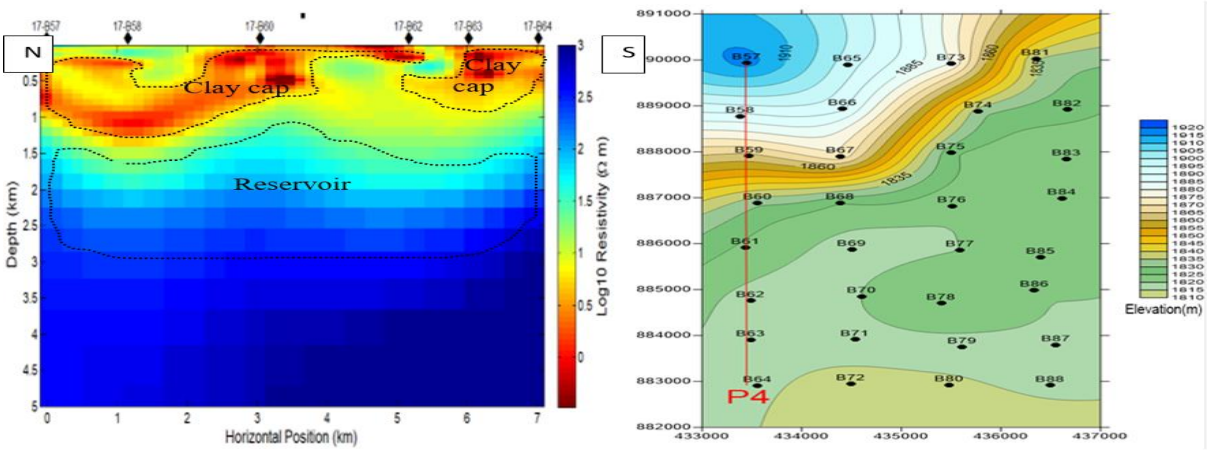

Figure 15. 2DOccam model along the profile p4

5 Conclusions and Recommendations

From the result of the survey, the following conclusions and recommendations have been made: (a) The MT method detected a low resistive surface layer (< 10 Ωm) of up to about1.5 km depth, this can be correlated with alteration zones caused by geothermal activity or lacustrine sediments or hydrothermally altered clay cap. (b) Below this low resistive layer resistivity is increasing up to (10-60 Ωm). This indicates an advancement to a possible reservoir at depth below about 1 km with a thickness of up to 1.5 km. (c) The faults have been detected on the profiles 1, 2 and 3, so it is strongly recommended to have addition MT/TEM (Transient Electromagneitc) profiles on this portion in order to understand the extension of the fault and reservoir (d) 3D MT survey is recommended (e) Gravity survey is also recommended to delineate the geological structure.

ACKNOWLEDGEMENTS

The authors highly appreciate and express their deep gratitude to the Geological Survey of Ethiopia and Mr. Solomon Kebede; director of geothermal resource exploration and assessment directorate for his untiring support and guidance. The authors wish to extend their appreciation to the UNEP/ARGeo for the technical assistance through experts to review the paper.

REFERENCES

Abera, B., and Mulugeta, N., (2017). One Meter Temperature Survey at the Butajira Geothermal Field. GSE, Ethiopia, Unpublished Internal Report, 17 pp.

Cagniard, L., (1953). Basic Theory of the Magneto-Telluric Method of Geophysical Prospecting. *Geophysics*, **18**, 605-635.

Hedlin, C. d., and Constable, S. (1990). Occam's Inversion to Generate Smooth: Two Dimensional Models from Magneto-Telluric Data. *Geophysics,* Vol. **55**, No. 12 (December 1990); P. 1613-1624, 10 Figs., 1 table.

Kebede, S., (2015). Geothermal Exploration and Development in Ethiopia: *Country Update,* (November 2015).

Pellerin, L., Johnston, J. M., and Hohman, G. W. (1996). A Numerical Evaluation of Electromagnetic Methods in Geothermal Exploration. *Geophysics,* 121-130.

Tikhnov AN (1950) The determination of the electrical properties of deep layers of earth's crust. Dokl Acad Nauk SSR **73**:295-297 (in Russian).

UNDP (1973): *Geology, geochemistry and hydrology of hot springs of the East African Rift System within Ethiopia*. UNDP, December report DD/SF/ON/11, NY.

Widodo and Saputera, D.H., 2016. Improving Levenberg-Marquardt Algorithm Inversion Result Using Singular Value Decomposition. Earth Science Research; Vol. **5**, No. 2; 2016.